A Thorough Review of Cooling Concepts and Thermal Management Techniques for Automotive WBG Inverters: Topology, Technology and Integration Level

Ekaterina Abramushkina [1,2,*], Assel Zhaksylyk [1,2], Thomas Geury [1,2], Mohamed El Baghdadi [1,2] and Omar Hegazy [1,2]

1   Mobility, Logistics and Automotive Technology Research Centre (MOBI), Department of Electrical Engineering and Energy Technology (ETEC), Faculty of Engineering, Vrije Universiteit Brussel (VUB), 1050 Brussel, Belgium; Assel.Zhaksylyk@vub.be (A.Z.); Thomas.Geury@vub.be (T.G.); Mohamed.El.Baghdadi@vub.be (M.E.B.); Omar.Hegazy@vub.be (O.H.)
2   Flanders Make, 3001 Heverlee, Belgium
*   Correspondence: Ekaterina.Abramushkina@vub.be

Abstract: The development of electric vehicles (EVs) is an important step towards clean and green cities. An electric powertrain provides power to the vehicle and consists of a charger, a battery, an inverter, and a motor as the main components. Supplied by a battery pack, the automotive inverter manages the power of the motor. EVs require a highly efficient inverter, which satisfies low cost, size, and weight requirements. One approach to meeting these requirements is to use the new wide-bandgap (WBG) semiconductors, which are being widely investigated in the industry as an alternative to silicon switches. WBG devices have superior intrinsic properties, such as high thermal flux, of up to 120 W/cm^2 (on average); junction temperature of 175–200 °C; blocking voltage limit of about 6.5 kV; switching frequency about 20-fold higher than that of Si; and up to 73% lower switching losses with a lower conduction voltage drop. This study presents a review of WBG-based inverter cooling systems to investigate trends in cooling techniques and changes associated with the use of WBG devices. The aim is to consider suitable cooling techniques for WBG inverters at different power levels.

Keywords: cooling system; wide-bandgap (WBG); silicon carbide (SiC); gallium nitride (GaN); automotive inverter; electric vehicle

1. Introduction

The electric vehicle (EV) market has grown rapidly for several decades as an alternative to conventional internal-combustion engine (ICE) vehicles, resulting in reduced air pollution [1]. The trend of reducing emissions in the atmosphere is demonstrated by the results of the voluntary agreement between the European Commission and the European Automobile Manufacturers Association (ACEA), the Japanese Automobile Manufacturers Association, and the Korean Automobile Manufacturers Association. This agreement has a target to reduce CO_2 emissions by at least 37.5% compared to a 2021 baseline, which equates to the reduction of CO_2 emissions to 59.4 g/km by 2030 (fleet-average emissions are tested through the New European Driving Cycle) [2,3]. Moreover, the European Union (EU) has set targets to reduce greenhouse emissions in the 2030 climate and energy framework to 55% compared to 1990 [3]. According to the ACEA, the percentage of electrically chargeable and hybrid cars compared to the total of all newly registered cars in Europe increased from 4.3% to 22.4% between 2017 and 2020 (Figure 1) [4].
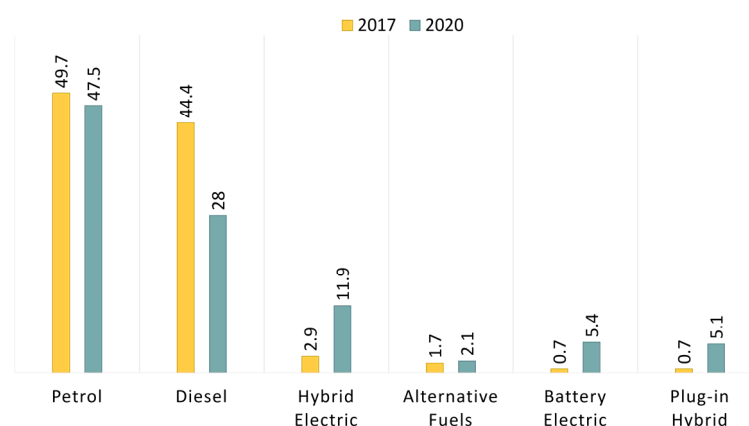
Figure 1. ACEA statistics: fuel types of new passenger cars in Europe, %.

The propulsion system plays a central role in providing tractive effort and energy management of an electric vehicle. The propulsion system includes the energy storage, power converters, electric motors, and associated controllers [5]. EV propulsion systems have been steadily improved, with the main development trends including higher power density, and reduction in size, weight, and cost [6]. The increase in power density and decrease in size can lead to poor heat dissipation and thermal stress, which in turn leads to additional failures of power converters [7]. Thus, to boost reliability, the main challenge of the propulsion's thermal management is to obtain a compromise between power density and size. This compromise allows thermal stress to be avoided and provides a better operating condition through a proper cooling system design [8].

Initially, cooling systems in EVs used forced air cooling, before evolving to liquid cooling as a more effective solution [9]. Because air cooling is less thermally efficient than liquid cooling, in current automotive applications the inverter air cooling is only possible for low power levels. Liquid cooling of EVs is usually provided using a low-temperature cooling loop (65 °C) for the power inverter [10,11], a high-temperature loop for the electric machine [12], and a separate battery-cooling loop (20–40 °C) [13–15]. This research focuses on the cooling design issues of automotive inverters with new wide-bandgap (WBG) semiconductors. Recent contributions regarding the advanced cooling of automotive inverters show two main approaches. The first approach is to eliminate the low temperature loop through high thermal performance cooling circuits, such as direct liquid cooling and dual-sided cooling. [13,16–19]. The second approach is to use air cooling for the inverter and machine, instead of separate cooling loops for each. An example is the integrated motor drive (IMD) [20]. The air-cooling loop for the IMDs requires the inverter to operate at high temperatures. Because the inverter operating temperatures are limited with silicon (Si) semiconductors, using new semiconductor materials may lead to wider applications of air cooling. WBG semiconductors are a possible substitution for Si semiconductors in automotive applications.

The thermal performance of a device can be evaluated using different parameters. The thermal resistance, R_{th}, is a parameter of power modules that indicates the heat transfer capability and determines the temperature difference between a heat source and a case or a heat sink, if specified. Therefore, the junction to heat sink thermal resistance value, R_{thj-h}, is a crucial parameter for heat dissipation efficiency. In addition, the design of power modules or cooling systems favors devices with a low R_{th} to maintain the junction temperature, T_j, within the acceptable range. The thermal resistance value is directly proportional to the material thickness (t) and inversely proportional to the thermal conductivity (σ) and dissipation area (A) [21–28].

High thermal performance of a power converter can be achieved in different ways, for example, using new materials with interesting thermal properties for power module manufacturing. Some of these materials can only be applied at manufacture, for example, new materials for substrates and semiconductors. Other thermal interface materials (TIMs)

can be chosen at the time of device development [29]. Due to their commercial availability, power modules can be used as inverter switches [8]. Another approach is to change the basic concepts of cooling. Examples of this approach are the design of new power module packages with reduced thermal impedance, and new hybrid (air–liquid) or integrated (at the power module or inverter level) cooling techniques [30]. Thus, cooling circuit design tends to apply new materials with the lowest thermal resistance and, at the same time, implement an optimal cooling architecture. Combining these approaches provides the highest power density and the most efficient cooling of the device.

WBG semiconductors have striking intrinsic properties and are currently widely available commercially [31,32]. The power electronic industry has adopted this type of semiconductor during the past decade. As a result, numerous studies about WBG inverter cooling have been conducted. This paper presents a review of different WBG inverter cooling approaches to examine the changes in cooling associated with WBG devices. The paper describes cooling techniques for automotive inverters as a part of EVs, and explores how the use of WBG semiconductors may result in more compact and effective cooling systems.

The paper is divided into eight sections. Section 2 describes new WBG semiconductors with a focus on their thermal properties. Section 3 details the classification of cooling approaches for automotive inverters. Sections 4 and 5 include examples of recent inverter air- and liquid-cooling implementations, respectively. Section 6 focuses on promising cooling techniques, which may soon attract more attention, related to WBG semiconductors. Section 7 is dedicated to summarizing the main research findings and highlighting trends in automotive inverter cooling systems. Section 8 presents the main conclusions.

2. Wide-Bandgap Semiconductors

WBG semiconductors are a promising alternative to Si semiconductors [32–37]. Because the WBG switches are commercially available in wide ranges of current and voltage ratings, this technology is mature enough to be used in industry [26,27,33,38,39]. Compared to Si devices, WBG devices have a number of superior physical properties, such as high thermal flux of up to 120 W/cm^2 (Si—10 W/cm^2); high junction temperature, T_{jmax}, of 175 to 200 °C (Si—T_{jmax} = 150 °C); high limit of blocking voltage (Si—maximum 6.5 kV); higher switching frequency (about 20-fold compared to Si); and lower switching losses (up to 73% lower) with a lower conduction voltage drop [40–42]. Spider diagrams comparing the parameters of Si with those of SiC and GaN are shown in Figure 2 [43]. Despite the advantages of WBG devices and their decreasing cost, it should be noted that they are still more expensive than conventional semiconductors [44].
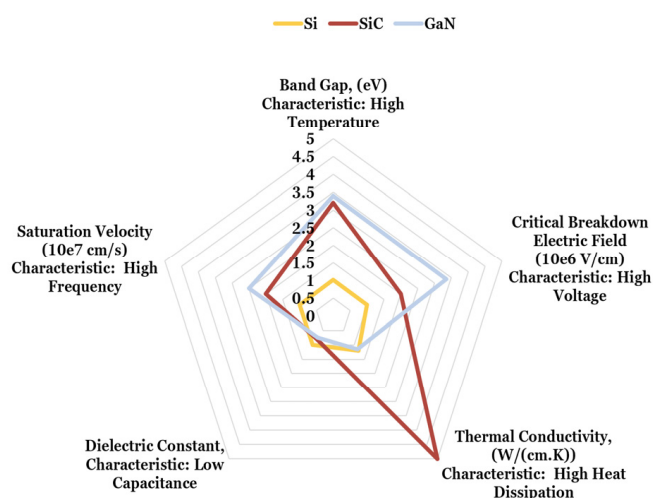

Figure 2. Parameter comparison of Si with respect to SiC and GaN, edited from [43].

The most developed and widespread WBG devices are those using gallium nitride (GaN) [45–48] and silicon carbide (SiC) [32,44,49–52] semiconductors. These two types of WBG devices are becoming increasingly popular in the field of EVs due to their higher blocking voltage, frequency, and operation temperature [53,54]. The growth in the market revenue of WBG devices can be seen from the Yole reports' road maps (see Figure 3) [55,56]. Despite the fact that the GaN semiconductors are considered to be suitable for use in automotive inverters, GaN technology does not currently have many commercially available high voltage modules compared to SiC [57–60]. Therefore, most of the examples in this paper are based on SiC inverters.
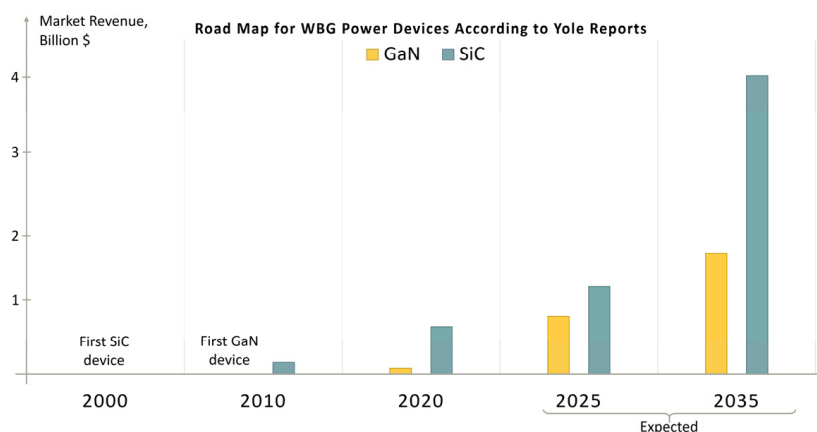

Figure 3. Road maps for WBG power devices according to Yole reports: SiC power devices and GaN power devices.

A previous study [61] using a WBG switch in a special high-temperature package with integrated microchannel liquid cooling showed results for peak power dissipation capability up to 5 kW/cm^2, i.e., significantly higher than that of a Si die. Theoretically, these advantages could lead to positive changes in the cooling of a power converter, for instance, by reducing the volume and production costs of the cooling system, combined with an increase in power density [44]. However, WBG technology is still constrained by limitations in its thermal packaging technology because of low thermal conductivity [62,63]. To increase operation temperatures up to the device's physical limitations (175–200 °C), high-temperature packaging should be designed. Examples can be found in the literature; for instance, Lu et al. presented a high-temperature packaged GaN High Electron Mobility Transistor (HEMT), which showed sufficient performance operating at 250 °C [64]. In addition, in 2020 Suganuma considered new highly conductive materials for interconnections inside a package to provide optimal thermal resistance at operating temperatures greater than 200 °C [65].

Due to their advantages, WBG devices have good thermal performance properties that can justify optimization or downgrading of an application's existing cooling system, for instance, using cheaper air cooling instead of liquid cooling. Overall, this can lower the volume and cost of EV powertrains, which is the main trend in the EV industry. As an example, in 2011 Zhang H. et al. [53] performed an extensive comparison of Si and SiC inverters. As a result, the fuel-to-wheel efficiency of hybrid electric vehicles (HEVs) was increased by 4.8% due to better regenerative braking. Fuel usage decreased from 3.94 to 3.36 L/100 km, which is consistent with an equivalent fuel economy improvement of about 13.8%. The efficiency of plug-in hybrid electric vehicles (PHEVs) increased by 13.8%, and the average electricity consumption during the Urban Dynamometer Driving Schedule (UDDS) drive cycle was reduced from 425.1 to 308.1 J/m, representing a decrease of 27.5%, due to the use of SiC switches. In addition, trends in EV inverters, as suggested by Zeng et al. in 2020, show that WBG inverters have had a higher peak power and power density compared to Si devices during the past decade [18].

3. Classification of Existing Cooling Techniques

The cooling of the inverter aims to provide an acceptable junction temperature of the power semiconductors during operation. Operating at acceptable temperatures increases the reliability and efficiency of the device. The cooling systems for automotive inverters have adopted numerous different architectures and solutions (Figure 4). Research on gas-cooled inverters, for example, can be found in Chintamani's paper [66]. Nevertheless, two fundamentally different approaches can be considered in inverter cooling: air and liquid cooling.
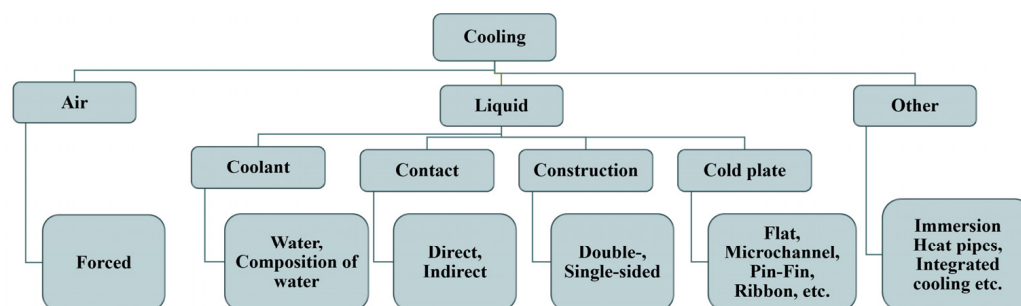

Figure 4. Classification of cooling techniques for automotive inverters.

Air cooling can be divided into forced and non-forced. The main advantages of air cooling are the implementation simplicity and low cost. Until recently, there has been little interest in air cooling for automotive inverters because the overall efficacy of this form of cooling is lower than that of liquid cooling. Thus, liquid cooling is a more popular and widespread solution. However, the emergence of WBG semiconductors with the ability to operate at higher temperatures has increased the interest in air cooling. Forced air cooling provides the principal operation efficiency with cheaper and easier cooling (see Section 4). Non-forced air cooling is not used in automotive applications because of the low heat dissipation capability.

Liquid cooling can be classified on basis of water-based or non-water-based coolant liquids. Water cooling is the simplest and most popular approach for automotive inverters, and non-water cooling usually implies that the driving motor in EVs uses oil cooling [67–70]. With regard to automotive inverter cooling, non-water cooling involves the use of water composites and has a special application in liquid cooling. The most popular water composite coolant is 50% water and 50% ethylene glycol [71] (see Section 5).

Regarding the type of contact with the coolant, liquid cooling can be categorized into direct and indirect cooling. Indirect cooling is an approach in which the power module has no direct contact with the liquid. As can be seen from Figure 5a, a conventional packaging scheme for indirect cooling includes a power device mounted through the solder over a ceramic substrate. A commonly used substrate is direct bonded copper (DBC). The substrate, in turn, is placed through DBC solder on the base plate (Cu, AlSiC, etc.). Electrical interconnections are provided via wire bonds. The entire construction is located on the heat sink or cold plate through TIMs to ensure heat dissipation [8]. All of these material and layer configurations affect the final thermal resistance. The difference between the direct and indirect liquid cooling is show in Figure 5. In direct liquid cooling, the base plate, TIM, and heat sink are replaced with only a base plate, thus reducing the number of layers inside the module (Figure 5b); as a result, the thermal resistance decreases. For instance, Mcpherson et al. (2017) compared the thermal resistance of three module configurations: (a) indirect cooling with a conventional flat cold plate; (b) direct cooling with a soldered pin-fin cold plate; and (c) direct cooling with a silver sintered pin-fin cold plate. The latter configuration almost halved the thermal resistance compared with indirect cooling [72]. In the case of indirect cooling, the thermal conductivity of the base plate, TIM, and heat sink play a key role in the overall heat dissipation capability [8,21,35,73]. The direct cooling approach involves eliminating the cold plate or heat sink, in addition to the

TIMs, and placing the power module in direct contact with water through the base plate only [72,74].
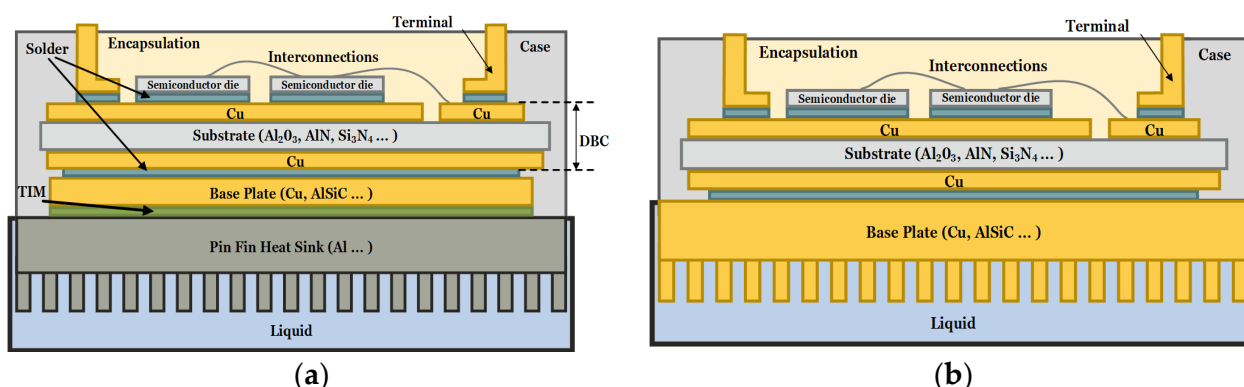

Figure 5. Schematic module representation with liquid cooling and pin fins: (**a**) indirect cooling; (**b**) direct cooling.

From the construction perspective, there are single-sided (Figure 6a) and double-sided (Figure 6d) liquid cooling systems [54]. In single-sided cooling, the power module is cooled only from one side. The standard single-sided cooling method uses a power module with a cold plate attached to the base plate trough the thermal interface materials [75,76]. Double-sided cooling involves changing the module construction in such a manner that two substrates are assembled one above the other with the power devices embedded between them [77]. The double-sided design allows the cooling efficiency to be increased because twice as much heat can be dissipated [28,78]. In addition, the bonding wires inside the module can be eliminated, which improves reliability [76]. The double-sided technique can be an efficient solution because the dissipation of power from both of the semiconductor's surfaces leads to a reduction in thermal impedance of up to 30% [79].
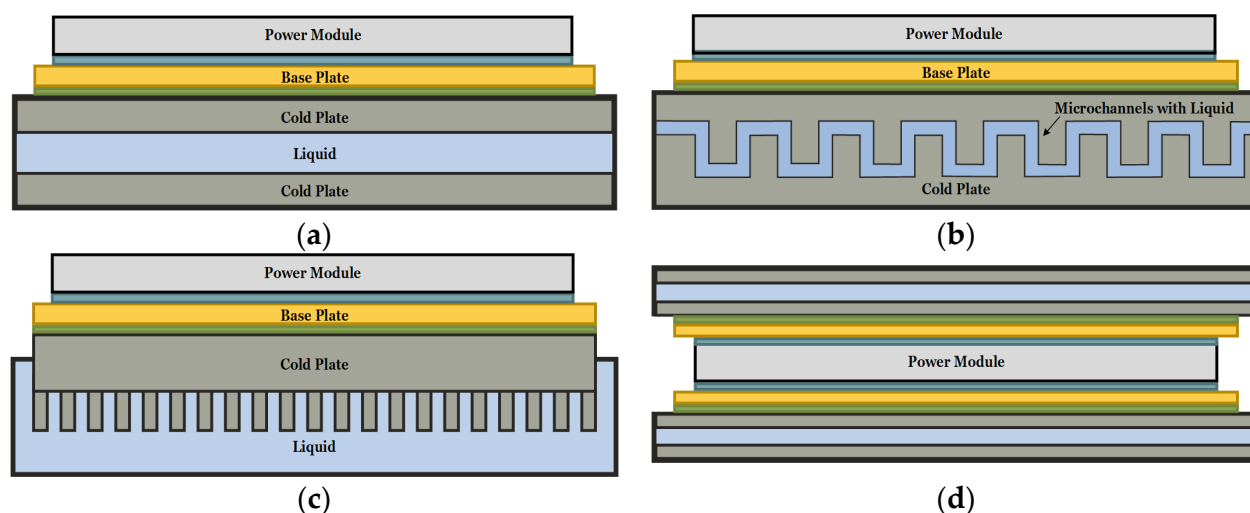
Figure 6. Single-sided cold plates: (**a**) flat; (**b**) microchannel; (**c**) pin fin; (**d**) power module for double-sided cooling.

The cold plate configuration, when applicable, can affect the heat dissipation capability of a power module. The dissipation capacity is related to the heat dissipation surface, which is usually determined by the cold plate surface area. The more common structures of cold plates are flat, multiple channel, microchannel, and pin fin (Figure 6). Regarding direct liquid cooling, when the cold plate is eliminated, the base plate can fulfill the functions of the cold plate and can also be implemented in different configurations.

In addition to standard air and liquid cooling, several other cooling techniques can be used for WBG inverters (see Section 6). These inverters have a smaller chip size but operate at higher temperatures. From the cooling system design perspective, this implies the use of hot and small areas to dissipate heat. Hoque et al. (2020) presented a modular heat sink for enhanced thermal performance of GaN switches [80]. Another approach to increasing the thermal performance of a small chip is to use an electric field technology; an example for GaN transistors can be found in [81]. Heat pipes may be a solution when some area require a higher heat dissipation capability. A jet impingement technique is also considered to be an effective cooling approach for automotive inverter applications [82]. Moreover, immersion cooling allows high heat transfer coefficients ($h > 2\ \mathrm{kW/(m^2 \cdot K)}$) to be achieved for the entire cooling system [83]. The basic principle of an immersion cooling technique is the submergence of the power modules in a thermally and not electrically conductive liquid [84]. In addition, integrated motor drive (IMD) topologies are currently gaining attention. Because of its proximity to the motor, the integrated inverter should work at higher temperatures. Therefore, WBG inverters, which have higher operating temperatures, are suitable for integration with the electrical machine. However, the proper cooling design of the integrated system remains important, as shown in recent studies [85].

4. Air Cooling

Air cooling is the simplest and cheapest cooling approach. The main problem with air cooling is a low heat flux. As a result, this technique is only suitable for low power applications. However, the high rated temperature and thermal flux dissipation capability of WBG semiconductors can compensate for the low flux of air cooling. Although the power density of the liquid-cooled SiC inverters is higher than that of the Si inverters, a liquid-cooling system implies additional components, which increase the volume and reduce the overall power density. Thus, the air-cooling system, which is the simplest implementation, can increase the power density of the inverter [18]. Hensler et al. (2017) proposed an unusual air-cooled inverter configuration, in which the heat sink has the shape of a hexagon, and the inner volume of the heat sink is separated by a plastic tube as an air path, resulting in a very compact solution. The principle of the hexagon heat sink is depicted in Figure 7a [86]. Another example was developed by Liu et al. using 3D air-cooled SiC packaging for a 20 kW inverter (see the concept in Figure 7b) [87]. The research of Li et al. (2020) showed an air-cooled 500 kW modular inverter with a conventional heat sink, in which the efficiency of the inverter was about 98.74% [88].

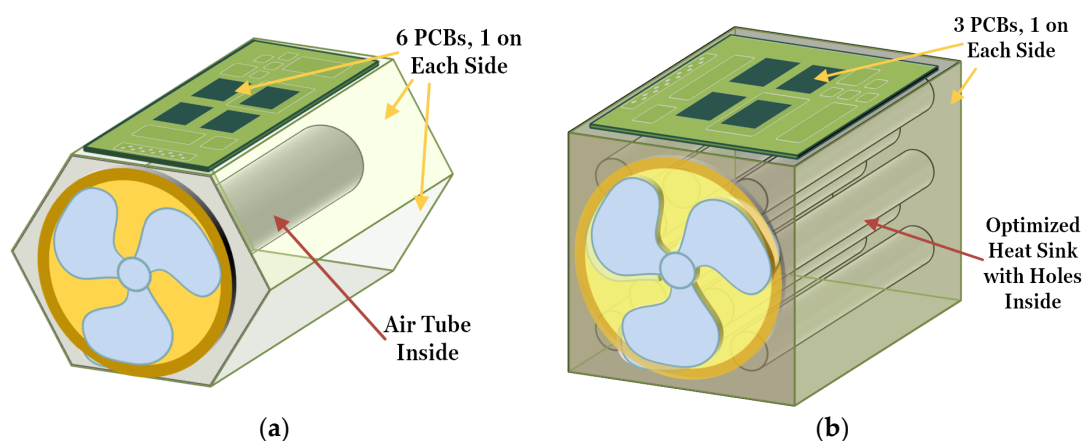**Figure 7.** Concepts of volumetric heatsinks for air cooling: (**a**) hexagonal heat sink for an inverter; (**b**) 3D heat sink for a half-bridge power module.

Zeng et al. proposed a design of a light and compact EV inverter without a liquid cooling system. The highest temperature reached by the SiC MOSFET was 110 °C, which is the rated temperature of WBG semiconductors. It was also proved that the forced air-

cooling technique provides a thermal flux of 200 W/cm^2, and the SiC MOSFET module has its own heat flux of 120 W/cm^2, which is 10-fold higher than that of the Si alternative. The high heat flux of the WBG module means that heat can be more easily dissipated from the chip surface. Thus, the smaller heat flux of air cooling, compared to liquid cooling, is sufficient for WBG power converters. Moreover, the optimized design of the Al heat sink reduces the thermal resistance of the heatsink from 0.44 to 0.35 K/W [18].

Another air-cooled SiC inverter was introduced by Wang et al. (2019), in which the power module was cooled with a thermally optimized heat sink (the principle is shown Figure 8). The optimized heat sink was generated using a MATLAB Genetic Algorithm (GA) and manufactured using 3D printing technology. This comprehensive heat sink allows sufficient heat to be dissipated from the semiconductors to enable the use of air cooling rather than liquid cooling. Moreover, two modules in one phase were split into two submodules, i.e., a top-side module and a bottom-side module, attached to two separate heat sinks, which were placed one above the other for better heat dissipation. Thermal optimization resulted in a reduction in the volume of the heat sink of 27% and reduced the junction temperature from 108.3 to 102.1 °C [89].
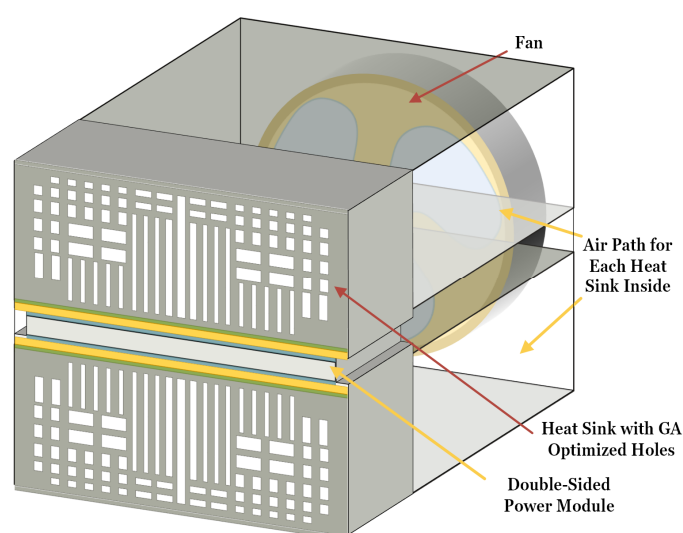

Figure 8. Principle of a GA-optimized heat sink for air cooling of a double-sided power module.

5. Liquid Cooling

Liquid cooling is currently the best option for EVs because of higher thermal transfer capability compared to air. Moreover, for power levels applied to automotive inverters, liquid cooling has proven effectiveness, which justifies the cost and challenges in implementation [74]. Indirect liquid cooling with flat cold plate is a mature technology and can now be found in the literature as a "conventional" or "standard" structure (with $R_{th} \geq 0.8$ K/W). Direct and indirect liquid cooling structures with complex cold plates are more advanced topologies [73]. Nevertheless, the use of the direct liquid cooling approach has increased because it shows the best thermal performance. By eliminating some layers of the power module solution, such as the TIM layer and the cold plate, the direct cooling approach allows the thermal resistance of the power module to be reduced by up to 30% [90]. Among the wide range of direct liquid cooling approaches, jet impingement (0.44–0.48 K/W), turbulator (0.2–0.55 K/W), and microchannel (0.13–0.24 K/W) technologies can be distinguished as major groups [91]. The direct liquid approach shows better thermal properties, such as a halving in the thermal resistance compared to indirect liquid cooling [92]. However, direct liquid cooling has a more complex implementation process, which results in higher costs. Thus, the application of direct liquid cooling is justified only to achieve higher thermal performance. It is worth noting that there can be a power module scale for power electronic devices, called integrated power module cooling, and a power converter

scale to evaluate the efficiency and thermal performance. In the following subsections, single-sided and double-sided cooling approaches are discussed for direct and indirect cooling implementation.

5.1. Single-Sided Cooling

Single-sided liquid cooling is still the most widespread and cost-effective solution for automotive inverters. At present, indirect liquid cooling development is represented by new structures of cold plates and heat sinks, where applicable. For instance, Mademlis et al. (2021) presented a heat sink with rectangular pin fins and optimized cooling channels [93]. The most common cold plate type for WBG inverters in recent contributions has a pin fin structure [94].

Qi et al. (2019) investigated a 30 kVA three-phase SiC inverter with a liquid-cooled cold plate for high-temperature operation. The inverter continuously operated for several hours in a high-temperature thermal chamber, where an ambient temperature of 180 °C was achieved. The maximum temperature of the commercial SiC modules, in the special high-temperature packaging, reached 150 °C, whereas the temperature of the cold plate and coolant were 85 and 50 °C, respectively [95]. In [96], a 100 kW SiC MOSFET three-phase inverter (34 kW/L) with a flat cold plate was tested at 105 °C ambient and 65 °C coolant temperatures. The thermal resistance from the junction to the coolant was 0.16 K/W, and the maximum die temperature was 113 °C. A two-level optimized cold plate was presented in Gurpinar et al. (2018) for a liquid-cooled 125 kW inverter, and the results showed a high thermal performance at a maximum operating capability of SiC-MOSFETs [97]. The two-level cold plate cools a power module and a DC link capacitor bank from different sides; this concept is depicted in Figure 9. Another example of cold plate thermal optimization can be found in Huber et al. (2018), in which six different SiC power modules were presented with a minimal thermal resistance of 0.331 K/W [98].
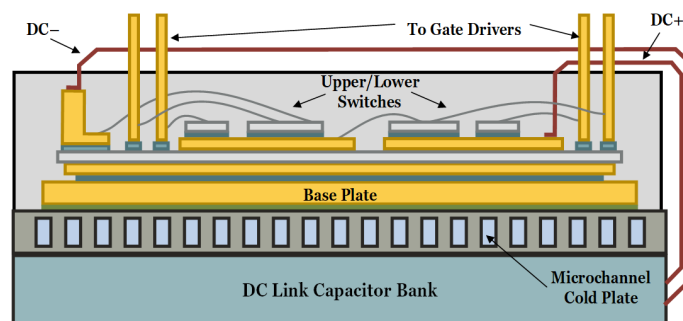

Figure 9. The principle of the two-sided cold plate for a module and DC link capacitors cooling.

Becker et al. carried out thermal optimization of a three-phase SiC MOSFET 1200 V 150 A automotive inverter with indirect liquid 50/50% water–glycol cooling and a copper heat sink with round pins. A cooling liquid circulates inside an aluminum case with a liquid pressure drop of 25 kPa at the pin area. The SiC power module with high conductivity Si_3N_4 (90 W/(m·K)) substrate was pressure contacted with a pin fin heat sink. The experiment included changing the number of parallel modules and the distance between them. It was found that if the distance between the chips was reduced from 8 to 1 mm, only three parallel SiC devices could be used rather than 4. The simulation of the complete assembled inverter showed that the junction temperature of the hottest chip was reduced from 226 to 154 °C with small temperature differences of $\Delta T = 5.1$ °C between the chips. Although 154 °C is still high, the maximum T_j of the SiC semiconductor used in this research was around 170 °C. Moreover, the hot spot temperature can be optimized by changing the inlet liquid temperature and flow. As a result, the design allowed the thermal resistance to be reduced by 32.1% [99].

5.2. Double-Sided Cooling

Double-sided liquid cooling is considered for motor driving applications. For instance, in 2020 Liu et al. [100] presented double-sided cooling of the SiC power module, and Möller et al. [92] suggested a double-sided cooling concept for an automotive application. Moreover, a double-sided liquid cooling module with jet impingement was reported in Tang et al. [101].

Catalano et al. [28] carried out an investigation of SiC-based power modules arranged in a half-bridge to prove the efficiency of double-sided cooling (the concept of the double-sided module is shown in Figure 10). To compare the thermal performance of single- and double-sided cooling, the thermal resistance was calculated for a wide range of boundary conditions. The heat transfer coefficient was used as a figure of merit for the boundary conditions; thus, $h = 101$ W/(m^2·K) means natural convection and $h = 109$ W/(m^2·K) indicates contact with an ideal heat sink. Moreover, two direct-bonded copper substrates based on Si_3N_4 and AlN were compared. According to the research results, double-sided cooling shows lower thermal resistance only when a high heat transfer coefficient is achieved ($h > 106$ W/(m^2·K)). In the case of the high heat transfer coefficient and the AlN type of substrate, the reduction of thermal resistance was up to 70%. It should be noted that the cost of the AlN substrate is high; thus, using this substrate is justified only if highly efficient cooling is needed.
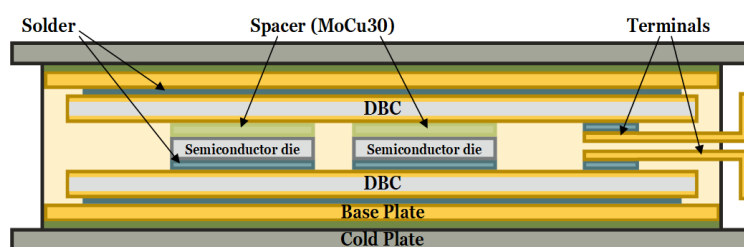

Figure 10. Schematic double-sided module representation.

In 2018, Hitachi's Research & Development Group developed a full-bridge SiC automotive inverter with an improved thermal design. According to the research result, the double-sided liquid cooling application ensured a 35% reduction in thermal resistance with a final value of about 0.175 K/W. Moreover, the double-sided structure enabled a solution to be derived for the issue that occurs when the parallel connections of semiconductors are required to share a large output current. In common structures, in which all interconnections are implemented via Al wires, the imbalance in the current can be considerable, especially when the switching frequency is high. A chip-connecting structure was built to provide an isometric current pattern, leading to a reduction in the current deviation between each chip from 10% to 2%. As a result, the overall design was able to reduce power losses by 60% in comparison to the conventional single-side cooled silicon modules [76].

6. Other Promising Cooling Approaches

The tendency toward higher powers and smaller sizes requires more efficient cooling with high heat flux. Although WBG devices differ from Si devices in terms of a large number of parameters, the most significant in terms of cooling are the smaller chip size and high heat flux due to the intrinsic material properties. When combined, these two properties are challenging for a cooling system, because it should dissipate a greater amount of heat from a smaller size. To ensure uniform temperature distribution, a cooling system should have high dissipation capability. WBG semiconductors become "hot points" during unbalanced temperature distribution, which lowers the reliability of the entire device. Thus, the WBG inverters' cooling requires a high cooling capacity and homogenous temperature maintenance of the power modules' chips. This section presents cooling techniques and approaches that provide a high thermal performance and may be successfully applied to emerging WBG power electronics systems.

New materials could be used to enhance the heat dissipating ability and provide a balanced temperature distribution. The use of metal foam for a heat sink, for instance, was presented by Lee et al. with Samsung Electronics Co in 2020. The authors investigated two heat sink structures: a metal foam (Type 1), and a metal foam with a pin fin baseplate (Type 2) for high power IGBTs. The concept of a metal foam layout in a power module is shown for Type 1 and Type 2 in Figure 11a and 11b, respectively. Porous heat sinks provide better heat transfer with a low-pressure drop in comparison to a microchannel technology, which usually requires pressure drops of 30–100 kPa [102]. The presented liquid cooling design provides a low R_{th} = 0.185 K/W and a low inlet pressure P_{in} = 5–15 kPa. Although the results were presented for IGBTs, the high thermal flux capability of porous heat sinks makes this technology suitable for WBGs. For instance, Takai et al. (2017) suggested the use of a porous heat sink for a GaN-based inverter [103].
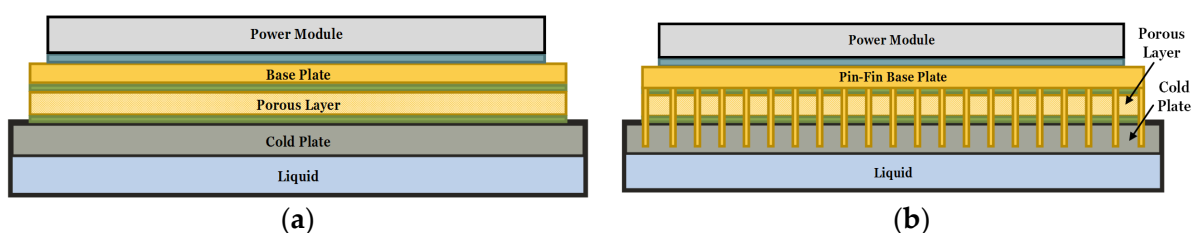

Figure 11. Concept of a metal foam layout in a power module: (**a**) a Type 1 structure; (**b**) a Type 2 structure.

The optimal structure of a cold plate can also increase the heat transfer capability of the device. Cold plates with direct single-sided liquid cooling have a higher thermal performance and simpler implementation process compared, for example, to double-sided modules. Thus, to design highly effective cooling for a WBG inverter, complex cold plate structures can be used. The simplest approach to enhance the effectiveness of a cold plate or base plate is to develop a structure with a larger surface for heat removal. In 2018, for instance, Infineon Technologies presented the liquid direct cooled Hybrid-PACKTM with different base plate structures. The thermal experiment included the measurement of three cold plate types: ribbon-bonded (this concept is depicted in Figure 12), pin fin, and flat. At the flow rate of 10 l/min, the result for the flat plate was R_{th} = 0.153 K/W, for the ribbon bonded plate R_{th} = 0.132 K/W, and for the pin fin structure R_{th} = 0.125 K/W [73]. Despite the fact that the thermal resistance of the pin fin cold plate was lower, the difference was not large (about 5.6%), and the manufacture of a ribbon-bonded cold plate is simpler and cheaper [90].
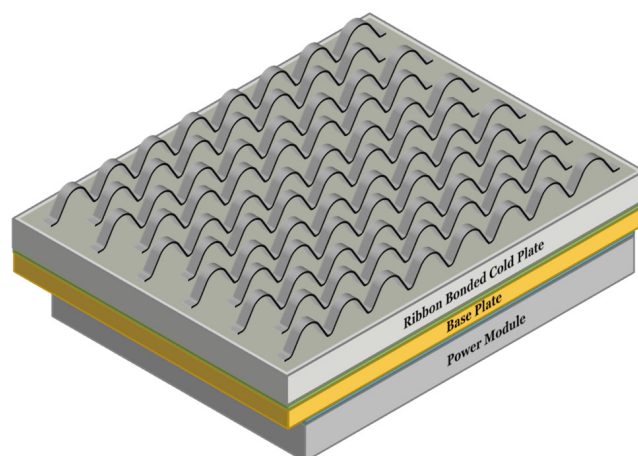

Figure 12. Concept of a ribbon-bonded cold plate.

Heat pipes are passive two-phase heat transfer devices. This cooling approach includes an evaporator, a condenser, a vapor line, a liquid line, and a vapor-removal channel [61]. It should be noted, however, that two-phase cooling systems, in general, are more effective than single phase systems [104]. The operational principle of a heat pipe, as shown in Figure 13, is to dissipate the heat from small hot sources to larger areas through evaporation and condensation [105,106]. This circulation of liquid leads to an increased heat transfer and, most importantly, provides higher thermal uniformity [107]. The heat transfer capability of heat pipes is determined only by the cooling capacity of the refrigerant [79]. Moreover, adding heat pipes allows the same heat transfer level to be obtained from smaller devices [108]. Therefore, heat pipes in cooling systems are particularly suitable for WBG devices because they provide higher heat dissipation from small areas, leading to a better temperature distribution among power devices. For instance, Gupta et al. (2018) presented cold plates with embedded heat pipes that reduced the maximum temperature of the device by 37 °C and improved temperature distribution [108]. In addition, Chang et al. proposed a heat pipe integrated heat sink, which decreased the temperature of the heatsink by 6 °C and the thermal resistance between the coolant and chip junction 10-fold [109].
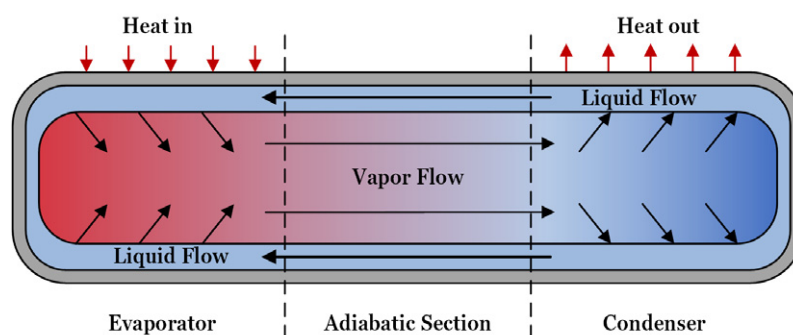

Figure 13. Working principle of a heat pipe.

Immersion cooling is one of the promising alternatives to conventional liquid cooling. This method consists of placing heat sources with direct contact in circulating liquid to dissipate the generated heat (the principle is shown in Figure 14). The most important requirement for immersion cooling systems is to use an electrically non-conductive working fluid, which allows homogenous cooling. Equal thermal distribution is crucial in terms of increasing the reliability for high power density power devices [104]. Potential types of fluids suitable for immersion cooling are de-ionized water, mineral oil, fluorocarbon-based fluids, and synthetic oil [83]. Immersion cooling, in general, is either single-phase or two-phase. The former includes using coolants only in one state of aggregation, and the latter implies physical state changes. This cooling approach has a higher heat transfer coefficient, which is important for increasing electrical power requirements, and can be implemented as one cooling loop for the inverter and motor in EVs, thus eliminating the main motor 105 °C coolant loop [68]. Yuki et al. (2020) presented an on-board two-phase immersion-cooled SiC inverter with a high heat flux of 500 W/cm^2, and showed that such a cooling technique can meet all of the requirements for automotive cooling because it is simple, compact, and highly effective [110].

The integrated motor drive (IMD) has emerged on the automotive powertrain market, and is rapidly evolving to become a key technology for compact and efficient motor drives [111]. Cooling technologies are being developed with integrated motor drives [85]. The recent literature has shown interest in WBG inverters for integrated solutions [112–115], in which air cooling can be applied for low-power motor drives. For instance, Dai et al. shared an air-cooled IMD concept in which the operation procedure of the air-cooling system is as follows: (1) inlet air is first drawn radially across the heat sink, which conducts heat out of the power modules; (2) the air is then pulled axially through the motor's airgap to cool the machine. A thermal finite element analysis showed the predicted temperature

distribution in the IMD with a current-source inverter (CSI) for steady-state operation at a rated load (3 kW) with 25 °C ambient air and an assumed air flow of 1.03×10^{-2} m³/s. The maximum efficiency of the inverter was 97.7% with a peak temperature of 107 °C for the WBG devices, and 96% for the machine with an inductor's peak temperature of 101 °C. These results show the feasibility of using air cooling for low-power IMD WBG-based solutions [13]. Another example of IMD cooling was presented in Lillo et al. in 2018. This is a liquid-cooled IMD in which each motor winding is connected to one power module through an innovative multilayer PCB structure, which is designed to minimize the space required for the end windings. The coolant first passes through the power section, and the stator windings are then immersed in the same coolant. This solution is based on a direct substrate cooling method with targeted impingement cooling, which can provide an extremely low specific thermal resistance. It can be concluded that some techniques, which are not widely used and rarely applied alone, may improve the efficiency of matured liquid cooling. In Lillo's study, the combination of spray cooling and immersion cooling provides effective liquid cooling in an IMD [14].
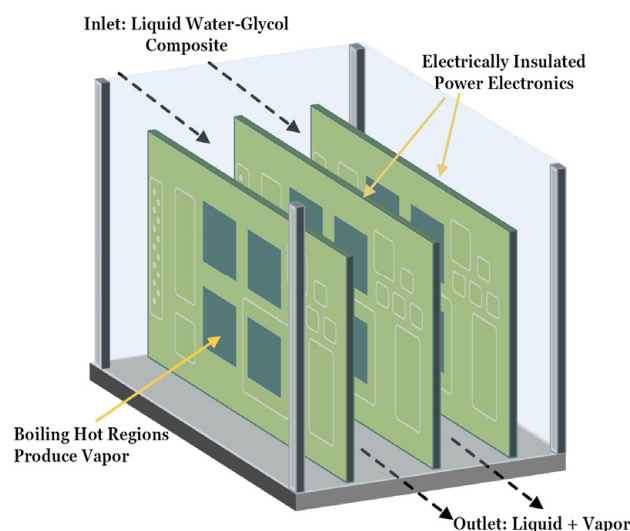
Figure 14. Immersion cooling principle.

7. Comparison of Cooling Techniques

WBG inverters operate at higher switching frequencies, power levels, and temperatures. The properties of WBG devices comply with increasing power levels and switching frequency requirements for power electronics devices. As shown by the literature review in this paper, the main advantages of WBG devices in cooling design are:

- The higher operating temperature of WBG devices leads to the design and use of simpler and cheaper cooling techniques;
- The higher switching frequencies and lower losses increase the overall efficiency of the device;
- The smaller size and higher heat flux of the WBG die is suitable for compact devices, although this is challenging for cooling system design because more heat should be dissipated from a smaller area.

A summary of cooling techniques and their application to WBG converters is shown in Table 1. Overall, both air- and liquid-cooled WBG inverters are presented with different optimized configurations of cold plates or heat sinks, with the purpose of increasing the heat dissipation capability of the device.

Table 1. Summary of reviewed cooling systems for WBG inverters.

Ref. No	Cooling	WBG Type	Power, kW /f$_s$, kHz	Heat Sink orCold Plate	Ambient T, °C /In. Coolant T, °C /In. Speed, l/min	T$_{jmax}$, °C	R$_{th}$, KW	Power Density, kW/L	Key Conclusions
[18]	Forced-air	1.2 kV/50 A SiC	10/50	Finned heat sink	25/-/-	140	j-amb. 0.35	13	The forced air cooling is feasible for the low power SiC inverter.
[86]	Forced-air	1.2 kV/75 A SiC MOSFET	2 × 27/100	Flat hexagonal heat sink	23/-/-	105	j-h.s. 1.0	17.2	The air-cooled hexagonal construction with a fan inside is a low inductivity, compact, and high-power density solution.
[87]	Forced-air	1.2 kV/120 A SiC	20/20	3D, 3-sided heatsink with air path pattern	25/-/-	106	-	18.6	The 3D SiC inverter with an integrated heat sink. The heat sink optimized through distribution and diameter of holes in an air path pattern.
[88]	Forced-air	1.2 kV/300 A SiC	5 × 100/20	Finned heat sink	40/-/-	133	j-amb. 0.071	1.25	Five 100 kW inverters paralleled to achieve a high efficiency 500 kW inverter.
[89]	Forced-air	1.7 kV SiC MOSFET	50/20	Finned heat sink	-/75/-	103	-	1.8	The GA-optimized heat sink allows an increase in the heat dissipation capability and decrease in the junction temperature.
[93]	Liquid	1.2 kV/450 A SiC	4/10	Cold plate, rectangular pins	105/65/10 water/ethylene	117	j-case 0.026	-	Short time overloading with 55% heat increase allows the heat sink temperature to be maintained beneath the limits.
[97]	Liquid	- SiC MOSFET	125/30	Micro-channel heat sink	105/65/10 water/ethylene	110	-	-	The manifold microchannel (MMC) heat sink is made of a high thermal conductivity material and exploited in the dual-sided heat sink design. The second side cools the capacitors.
[94]	Liquid	1.2 kV/450 A SiC MOSFET	30/20	Pin-fin cold plate	140/105/10 water/ethylene	-	-	17	The inverter is designed for operating at a high ambient temperature. The coolant temperature is considered to be 105 °C to use a single cooling loop for the inverter and motor.
[95]	Liquid	1200 V/300 A SiC MOSFET	30/10	Commercial cold plate	180/50/- water/ethylene	150	j-case 0.2	-	The inverter showed satisfying operating performance at the 180 °C ambient temperature because the high-temperature SiC packaging was used.
[96]	Liquid	- SiC MOSFET	100/40	62 mm wide, 007-MXQ-01 cold plate	105/65/10	113	j-case 0.16	34	A high-power density liquid-cooled inverter is presented.
[76]	Liquid	- SiC MOSFET	-/12	Double-sided cold plate	-	150	j-cool. 0.17	-	The double-sided cold plate with the direct liquid approach allows the thermal resistance from the junction to coolant to be decreased by 35%.

Air cooling is a cheaper and simpler solution compared to liquid cooling. Liquid cooling requires additional auxiliaries (pumps, radiator, compressor, and chiller), which increase the weight and volume of the system. Because of higher working temperatures and heat flux of WBG devices, air cooling can be applied to a wider power range of inverters compared to Si devices. As can be seen from recent studies, introducing WBG devices on the market transformed the trend from liquid to forced air cooling for low-power (up to 50 kW) [89] and low power density (up to 18 kW/L) [87] applications. In addition, some studies are devoted to volume hexagonal or cubic air-cooled inverters. Such construction increases the power density of the inverter; for example, the standard construction with a common flat and finned heat sink achieves 13 kW/L [18] and both of the presented examples of volume inverters achieve 17.2 and 18.6 kW/L [86,87]. Another approach of applying air cooling for the power inverter is a modular inverter structure. Modular air-cooled inverters from [87,88] are solutions with high power levels. Due to the use of separated modules, each module-inverter has a low power level and can be air cooled.

Nevertheless, liquid cooling is still the most widespread solution for power electronics applications in EVs, and indirect liquid cooling is still feasible. Single-sided indirect cooling is developing via improvement of the cold plate, as can be seen in [93,94]. Moreover, the single-sided direct and indirect cooling for WBG inverters has been optimized in two ways: by changing the distance between the chips and changing the number of power switches [96–99]. Because WBGs have a smaller chip size, additional power switches can be used without an increase in the volume of the device, to provide better current sharing in one inverter leg as more parallel chips are used. From the thermal optimization perspective, in contrast, the reduced number of chips enables a larger distance between them. When chips have a larger distance between them, applied cooling has better heat dissipation capability and temperature distribution. The main drawback of this optimization is the increase in the operating current for each power switch. However, in the case of WBG semiconductors, this problem can be compensated for by using higher rated currents of WBGs. The double-sided cooling approach shows good thermal properties; for example, reduced thermal resistance up to 35% [28]. Such cooling is suitable for high thermal performance and high temperature solutions. Although the heat dissipation capability of the cooling system is low, double-sided cooling does not justify the complexity of its implementation. In addition, power modules with double-sided cooling have higher reliability due to the replacement of the bonding wires by more reliable interconnectors. Furthermore, the double-sided power module can be designed for an optimized current path between parallel modules [76].

8. Conclusions

This paper provides a technical assessment and review analysis of the cooling technologies for automotive WBG inverters. The WBG semiconductors, classification of cooling techniques, and details of each cooling technique are reviewed in detail. These semiconductors have different intrinsic properties that can affect the thermal properties of the overall system.

WBG technology is a highly promising solution for the next generation of power electronics and automotive powertrains due to their superior intrinsic characteristics, such as high thermal flux, available junction temperature, limit of the blocking voltage, and switching frequency, and low switching losses and conduction voltage drop.

The commercial availability of WBG devices enables the use of cheaper and simpler air-cooling approaches for low-power motor drives up to 50 kW, rather than liquid cooling. Two main approaches aimed at increasing the heat dissipation capability of air cooling can be highlighted: the volume and the modular design of power inverter. Whereas the former provides a compact inverter with a larger surface to dissipate heat, the latter modular design provides all of the required power of the device divided between separate modules, in which each module has lower power and can be cooled using the forced-air approach.

Liquid cooling remains the most cost-effective solution for a wide range of power levels. Numerous studies have been conducted on the different optimization approaches, which include new shapes of cold plates or heat sinks, the use of new materials, and the combination of two or more cooling techniques. Single-sided indirect liquid cooling remains highly popular and shows good thermal performance, particularly when new WBGs with better thermal properties are applied. Because WBGs have a smaller chip size, smaller losses, and a higher rated current and voltage, some studies suggest thermal optimization can be achieved by changing the number of semiconductors in one inverter leg and by changing the distance between the power switches. Direct liquid cooling has better thermal performance than indirect cooling, but adds complexity to the implementation. Such a cooling approach can be useful for high performance and high temperature solutions. Indirect and direct double-sided cooling are applicable for devices with a high heat transfer coefficient, because only in this case is their implementation complexity justified.

According to the trend of increasing rated power levels of power inverters, high heat flux systems, such as immersion cooling, may soon become widespread. Moreover, WBG power modules, in the case of high power levels of the device, need to be cooled with special cooling approaches, which are capable of effectively dissipating heat from a small hot area. A porous heat sink, heat pipes, and special thermal packaging may be a solution. In addition, high operating temperatures of WBGs also provide an opportunity for the use of IMDs with a shared motor and inverter cooling.

Due to the growing demand for increasing power levels in motor drives, cooling technology is an important part of the system. The results of this paper could be used for many future studies on the topic.

Author Contributions: Conceptualization, E.A.; resources, A.Z., T.G., M.E.B.; writing—original draft preparation, E.A.; writing—review and editing, A.Z., T.G., M.E.B.; visualization, E.A.; supervision, O.H. All authors have read and agreed to the published version of the manuscript.

References

1. Giampieri, A.; Ling-Chin, J.; Ma, Z.; Smallbone, A.; Roskilly, A.P. A Review of the Current Automotive Manufacturing Practice from an Energy Perspective. *Appl. Energy* **2020**, *261*, 114074. [CrossRef]
2. Dieselnet, 2020, Emission Standarts: Europe: Cars: Greenhouse Gas Emissions. Available online: https://dieselnet.com (accessed on 26 November 2020).
3. An Official Website of the European Union. European Commission. Climate Strategies & Targets. Available online: https://ec.europa.eu/clima/policies/strategies_en (accessed on 26 November 2020).
4. ACEA. European Automobile Manufacturers Association. 2019. Available online: https://www.acea.be (accessed on 26 November 2020).
5. Rajashekara, K. Present Status and Future Trends in Electric Vehicle Propulsion Technologies. *IEEE J. Emerg. Sel. Top. Power Electron.* **2013**, *1*, 3–10. [CrossRef]
6. Reimers, J.; Dorn-Gomba, L.; Mak, C.; Emadi, A. Automotive Traction Inverters: Current Status and Future Trends. *IEEE Trans. Veh. Technol.* **2019**, *68*, 3337–3350. [CrossRef]
7. Hazra, S.; De, A.; Cheng, L.; Palmour, J.; Schupbach, M.; Hull, B.A.; Allen, S.; Bhattacharya, S. High Switching Performance of 1700-V, 50-A SiC Power MOSFET over Si IGBT/BiMOSFET for Advanced Power Conversion Applications. *IEEE Trans. Power Electron.* **2016**, *31*, 4742–4754. [CrossRef]
8. López, I.; Ibarra, E.; Matallana, A.; Andreu, J.; Kortabarria, I. Next Generation Electric Drives for HEV/EV Propulsion Systems: Technology, Trends and Challenges. *Renew. Sustain. Energy Rev.* **2019**, *114*, 109336. [CrossRef]
9. Kang, S.S. Advanced Cooling for Power Electronics. In Proceedings of the 2012 7th International Conference on Integrated Power Electronics Systems (CIPS), Nuremberg, Germany, 6–8 March 2012; pp. 1–8.
10. Behi, H.; Karimi, D.; Behi, M.; Jaguemont, J.; Ghanbarpour, M.; Behnia, M.; Berecibar, M.; van Mierlo, J. Thermal Management Analysis Using Heat Pipe in the High Current Discharging of Lithium-Ion Battery in Electric Vehicles. *J. Energy Storage* **2020**, *32*, 101893. [CrossRef]

11.　Li, W.; Peng, X.; Xiao, M.; Garg, A.; Gao, L. Multi-Objective Design Optimization for Mini-Channel Cooling Battery Thermal Management System in an Electric Vehicle. *Int. J. Energy Res.* **2019**, *43*, 3668–3680. [CrossRef]

12.　Gai, Y.; Kimiabeigi, M.; Chuan Chong, Y.; Widmer, J.D.; Deng, X.; Popescu, M.; Goss, J.; Staton, D.A.; Steven, A. Cooling of Automotive Traction Motors: Schemes, Examples, and Computation Methods. *IEEE Trans. Ind. Electron.* **2019**, *66*, 1681–1692. [CrossRef]

13.　Dai, H.; Jahns, T.M.; Torres, R.A.; Liu, M.; Sarlioglu, B.; Chang, S. Development of High-Frequency WBG Power Modules with Reverse-Voltage-Blocking Capability for an Integrated Motor Drive Using a Current-Source Inverter. In Proceedings of the 2018 IEEE Energy Conversion Congress and Exposition (ECCE), Portland, OR, USA, 23–27 September 2018; pp. 1808–1815. [CrossRef]

14.　de Lillo, L.; Ahmadi, B.; Empringham, L.; Johnson, M.; Espina, J.; Abebe, R. Next Generation Integrated Drive, NGID: A Novel Approach to Thermal and Electrical Integration of High Power Density Drives in Automotive Applications. In Proceedings of the 2018 IEEE Energy Conversion Congress and Exposition (ECCE), Portland, OR, USA, 23–27 September 2018; pp. 1228–1232. [CrossRef]

15.　Alipour, M.; Hassanpouryouzband, A.; Kizilel, R. Investigation of the Applicability of Helium-Based Cooling System for Li-Ion Batteries. *Electrochem* **2021**, *2*, 11. [CrossRef]

16.　Murakami, Y.; Tajima, Y.; Tanimoto, S. Air-Cooled Full-SiC High Power Density Inverter Unit. In Proceedings of the 2013 World Electric Vehicle Symposium and Exhibition (EVS27), Barcelona, Spain, 17–20 November 2013; pp. 1–4. [CrossRef]

17.　Jia, X.; He, F.; Liu, C.; Hu, C.; Li, Y.; BORONKA, A.; Xu, D. Design of High Efficiency Inverter with Air Cooling for Electric Vehicle. In Proceedings of the 2018 IEEE International Power Electronics and Application Conference and Exposition (PEAC), Shenzhen, China, 4–7 November 2018; pp. 1–6. [CrossRef]

18.　Zeng, Z.; Zhang, X.; Blaabjerg, F.; Chen, H.; Sun, T. Stepwise Design Methodology and Heterogeneous Integration Routine of Air-Cooled SiC Inverter for Electric Vehicle. *IEEE Trans. Power Electron.* **2020**, *35*, 3973–3988. [CrossRef]

19.　Wrzecionko, B.; Bortis, D.; Kolar, J.W. A 120 °C Ambient Temperature Forced Air-Cooled Normally-off SiC JFET Automotive Inverter System. *IEEE Trans. Power Electron.* **2014**, *29*, 2345–2358. [CrossRef]

20.　Wang, Y.; Jones, S.; Dai, A.; Liu, G. Reliability Enhancement by Integrated Liquid Cooling in Power IGBT Modules for Hybrid and Electric Vehicles. *Microelectron. Reliab.* **2014**, *54*, 1911–1915. [CrossRef]

21.　Hou, F.; Wang, W.; Cao, L.; Li, J.; Su, M.; Lin, T.; Zhang, G.; Ferreira, B. Review of Packaging Schemes for Power Module. *IEEE J. Emerg. Sel. Top. Power Electron.* **2020**, *8*, 223–238. [CrossRef]

22.　Razeeb, K.M.; Dalton, E.; Cross, G.L.W.; Robinson, A.J. Present and Future Thermal Interface Materials for Electronic Devices. *Int. Mater. Rev.* **2018**, *63*, 1–21. [CrossRef]

23.　Pan, C.A.; Yeh, C.T.; Qiu, W.C.; Lin, R.Z.; Hung, L.Y.; Ng, K.T.; Lin, C.F.; Chung, C.K.; Jiang, D.S.; Hsiao, C.S. Assembly and Reliability Challenges for Next Generation High Thermal TIM Materials. In Proceedings of the 2017 IEEE 67th Electronic Components and Technology Conference (ECTC), Orlando, FL, USA, 30 May–2 June 2017; pp. 2033–2039. [CrossRef]

24.　Hansson, J.; Nilsson, T.M.J.; Ye, L.; Liu, J. Novel Nanostructured Thermal Interface Materials: A Review. *Int. Mater. Rev.* **2018**, *63*, 22–45. [CrossRef]

25.　Zhang, Y.; Heo, Y.J.; Son, Y.R.; In, I.; An, K.H.; Kim, B.J.; Park, S.J. Recent Advanced Thermal Interfacial Materials: A Review of Conducting Mechanisms and Parameters of Carbon Materials. *Carbon* **2019**, *142*, 445–460. [CrossRef]

26.　Morya, A.K.; Gardner, M.C.; Anvari, B.; Liu, L.; Yepes, A.G.; Doval-Gandoy, J.; Toliyat, H.A. Wide Bandgap Devices in AC Electric Drives: Opportunities and Challenges. *IEEE Trans. Transp. Electrif.* **2019**, *5*, 3–20. [CrossRef]

27.　Su, M.; Chen, C.; Sharma, S.; Kikuchi, J. Performance and Cost Considerations for SiC-Based HEV Traction Inverter Systems. In Proceedings of the IEEE 3rd Workshop on Wide Bandgap Power Devices and Applications (WiPDA), Blacksburg, VA, USA, 2–4 November 2015; pp. 345–350. [CrossRef]

28.　Catalano, A.P.; Scognamillo, C.; Castellazzi, A.; d'Alessandro, V. Optimum Thermal Design of High-Voltage Double-Sided Cooled Multi-Chip SiC Power Modules. In Proceedings of the 2019 25th International Workshop on Thermal Investigations of ICs and Systems (THERMINIC), Lecco, Italy, 25–27 September 2019; pp. 1–4. [CrossRef]

29.　Karimi, D.; Behi, H.; Jaguemont, J.; el Baghdadi, M.; van Mierlo, J.; Hegazy, O. Thermal Concept Design of MOSFET Power Modules in Inverter Subsystems for Electric Vehicles. In Proceedings of the 2019 9th International Conference on Power and Energy Systems (ICPES), Perth, WA, Australia, 10–12 December 2019; pp. 1–6. [CrossRef]

30.　She, X.; Huang, A.Q.; Lucia, O.; Ozpineci, B. Review of Silicon Carbide Power Devices and Their Applications. *IEEE Trans. Ind. Electron.* **2017**, *64*, 8193–8205. [CrossRef]

31.　Husain, I.; Ozpineci, B.; Islam, M.S.; Gurpinar, E.; Su, G.J.; Yu, W.; Chowdhury, S.; Xue, L.; Rahman, D.; Sahu, R. Electric Drive Technology Trends, Challenges, and Opportunities for Future Electric Vehicles. *Proc. IEEE* **2021**, *109*, 1039–1059. [CrossRef]

32.　Bérubé, Y.; Ghazanfari, A.; Fortin Blanchette, H.; Perreault, C.; Zaghib, K. Recent Advances in Wide Bandgap Devices for Automotive Industry. In Proceedings of the IECON 2020 The 46th Annual Conference of the IEEE Industrial Electronics Society, Singapore, 18–21 October 2020; pp. 2557–2564. [CrossRef]

33.　Millan, J.; Godignon, P.; Perpina, X.; Perez-Tomas, A.; Rebollo, J. A Survey of Wide Bandgap Power Semiconductor Devices. *IEEE Trans. Power Electron.* **2014**, *29*, 2155–2163. [CrossRef]

34.　Lee, H.; Smet, V.; Tummala, R. A Review of SiC Power Module Packaging Technologies: Challenges, Advances, and Emerging Issues. *IEEE J. Emerg. Sel. Top. Power Electron.* **2020**, *8*, 239–255. [CrossRef]

35. Chen, C.; Luo, F.; Kang, Y. A Review of SiC Power Module Packaging: Layout, Material System and Integration. *CPSS Trans. Power Electron. Appl.* **2017**, *2*, 170–186. [CrossRef]

36. Nitzsche, M.; Cheshire, C.; Fisher, M.; Ruthardt, J. Comprehensive Comparison of a SiC MOSFET and Si IGBT Based Inverter. In Proceedings of the PCIM Europe 2019 International Exhibition and Conference for Power Electronics, Intelligent Motion, Renewable Energy and Energy Management, Nuremberg, Germany, 7–9 May 2019; pp. 1828–1834.

37. Nisch, A.; Heller, M.; Wondrak, W.; Bucher, A.; Hasenohr, C.; Kefer, K.; Lunz, B.; Pawellek, A.; Smit, A.; Gärtner, M.; et al. Simulation and Measurement-Based Analysis of Efficiency Improvement of SiC MOSFETs in a Series-Production Ready 300 KW / 400 V Automotive Traction Inverter. In Proceedings of the 2020 22nd European Conference on Power Electronics and Applications (EPE'20 ECCE Europe), Lyon, France, 7–11 September 2020; pp. 1–10. [CrossRef]

38. Matallana, A.; Ibarra, E.; López, I.; Andreu, J.; Garate, J.I.; Jordà, X.; Rebollo, J. Power Module Electronics in HEV/EV Applications: New Trends in Wide-Bandgap Semiconductor Technologies and Design Aspects. *Renew. Sustain. Energy Rev.* **2019**, *113*, 109264. [CrossRef]

39. Wen, X.; Fan, T.; Ning, P.; Guo, Q. Technical Approaches towards Ultra-High Power Density SiC Inverter in Electric Vehicle Applications. *CES Trans. Electr. Mach. Syst.* **2017**, *1*, 231–237. [CrossRef]

40. Ding, X.; Du, M.; Duan, C.; Guo, H.; Xiong, R.; Xu, J.; Cheng, J.; Luk, P.C.K. Analytical and Experimental Evaluation of SiC-Inverter Nonlinearities for Traction Drives Used in Electric Vehicles. *IEEE Trans. Veh. Technol.* **2018**, *67*, 146–159. [CrossRef]

41. Adan, A.O.; Tanaka, D.; Burgyan, L.L.; Kakizaki, Y. The Current Status and Trends of 1,200-V Commercial Silicon-Carbide MOSFETs: Deep Physical Analysis of Power Transistors From a Designer's Perspective. *IEEE Power Electron. Mag.* **2019**, *6*, 36–47. [CrossRef]

42. Allca-Pekarovic, A.; Kollmeyer, P.J.; Mahvelatishamsabadi, P. Comparison of IGBT and SiC Inverter Loss for 400V and 800V DC Bus Electric Vehicle Drivetrains. In Proceedings of the 2020 IEEE Energy Conversion Congress and Exposition (ECCE), Detroit, MI, USA, 11–15 October 2020; pp. 6338–6344. [CrossRef]

43. Chakraborty, S.; Vu, H.N.; Hasan, M.M.; Tran, D.D.; el Baghdadi, M.; Hegazy, O. DC-DC Converter Topologies for Electric Vehicles, Plug-in Hybrid Electric Vehicles and Fast Charging Stations: State of the Art and Future Trends. *Energies* **2019**, *12*, 1569. [CrossRef]

44. Mauromicale, G.; Raciti, A.; Rizzo, S.A.; Susinni, G.; Abbatelli, L.; Buonomo, S.; Cavallaro, D.; Giuffrida, V. SiC Power Modules for Traction Inverters in Automotive Applications. In Proceedings of the IECON 2019-45th Annual Conference of the IEEE Industrial Electronics Society, Lisbon, Portugal, 14–17 October 2019; pp. 1973–1978. [CrossRef]

45. Ding, H.; Li, Y.; Han, D.; Liu, M.; Sarlioglu, B. Design of a Novel Integrated Motor-Compressor Machine with GaN-Based Inverters. In Proceedings of the 2017 19th European Conference on Power Electronics and Applications (EPE'17 ECCE Europe), Warsaw, Poland, 11–14 September 2017; pp. 1–9. [CrossRef]

46. Ma, C.T.; Gu, Z.H. Review of GaN HEMT Applications in Power Converters over 500 W. *Electronics* **2019**, *8*, 1401. [CrossRef]

47. Keshmiri, N.; Wang, D.; Agrawal, B.; Hou, R.; Emadi, A. Current Status and Future Trends of GaN HEMTs in Electrified Transportation. *IEEE Access* **2020**, *8*, 70553–70571. [CrossRef]

48. Hassan, A.; Savaria, Y.; Sawan, M. GaN Integration Technology, an Ideal Candidate for High-Temperature Applications: A Review. *IEEE Access* **2018**, *6*, 78790–78802. [CrossRef]

49. la Manita, S.; Giuffrida, V.; Buonomo, S. Benefits and Advantages of Using SiC. In Proceedings of the PCIM Europe 2019; International Exhibition and Conference for Power Electronics, Intelligent Motion, Renewable Energy and Energy Management, Nuremberg, Germany, 7–9 May 2019; pp. 1419–1422.

50. Chou, W.; Kempitiya, A.; Vodyakho, O. Reduction of Power Losses of SiC MOSFET Based Power Modules in Automotive Traction Inverter Applications. In Proceedings of the 2018 IEEE Transportation Electrification Conference and Expo (ITEC), Long Beach, CA, USA, 13–15 June 2018; pp. 1035–1038. [CrossRef]

51. Nakanishi, M.; Hayashi, K.; Enomoto, A.; Hayashiguchi, M.; Ando, M.; Felgemacher, C.; Mashaly, A.; Richard, G. Automotive Traction Inverter Utilizing SiC Power Module. In Proceedings of the PCIM Europe 2018; International Exhibition and Conference for Power Electronics, Intelligent Motion, Renewable Energy and Energy Management, Nuremberg, Germany, 5–7 June 2018; pp. 1–6.

52. Yuan, X.; Laird, I.; Walder, S. Opportunities, Challenges, and Potential Solutions in the Application of Fast-Switching SiC Power Devices and Converters. *IEEE Trans. Power Electron.* **2021**, *36*, 3925–3945. [CrossRef]

53. Zhang, H.; Tolbert, L.M.; Ozpineci, B. Impact of SiC Devices on Hybrid Electric and Plug-in Hybrid Electric Vehicles. *IEEE Trans. Ind. Appl.* **2011**, *47*, 912–921. [CrossRef]

54. Tang, G.; Chai, T.C.; Zhang, X. Thermal Optimization and Characterization of Sic-Based High Power Electronics Packages with Advanced Thermal Design. *IEEE Trans. Compon. Packag. Manuf. Technol.* **2019**, *9*, 854–863. [CrossRef]

55. Power SiC: Materials, Devices and Applications. 2020. Available online: www.yole.fr (accessed on 10 April 2021).

56. GaN Power 2021: Epitaxy, Devices, Applications and Technology Trends. Available online: www.yole.fr (accessed on 3 May 2021).

57. Jordà, X.; Perpiñà, X.; Vellvehi, M.; Sanchez, D.; García, A.; Avila, A. Analysis of Natural Convection Cooling Solutions for GaN HEMT Transistors. In Proceedings of the 2018 20th European Conference on Power Electronics and Applications (EPE'18 ECCE Europe), Riga, Latvia, 17–21 September 2018; pp. 1–9.

58. Avila, A.; Garcia-Bediaga, A.; Gonzalez, F.; Jordà, X.; Perpiñà, X.; Rujas, A. Thermal Performance Analysis of GaN-Based High-Power Converters. In Proceedings of the 2018 20th European Conference on Power Electronics and Applications (EPE'18 ECCE Europe), Riga, Latvia, 17–21 September 2018; pp. 1–10.

59. Barth, C.B.; Assem, P.; Foulkes, T.; Chung, W.H.; Modeer, T.; Lei, Y.; Pilawa-Podgurski, R.C.N. Design and Control of a GaN-Based, 13-Level, Flying Capacitor Multilevel Inverter. *IEEE J. Emerg. Sel. Top. Power Electron.* **2020**, *8*, 2179–2191. [CrossRef]

60. Meng, W.; Zhang, F.; Fu, Z. A High Power Density Inverter Design Based on GaN Power Devices. In Proceedings of the 2018 8th International Conference on Power and Energy Systems (ICPES), Colombo, Sri Lanka, 21–22 December 2018; pp. 1–5. [CrossRef]

61. Aranzabal, I.; de Alegria, I.M.; Delmonte, N.; Cova, P.; Kortabarria, I. Comparison of the Heat Transfer Capabilities of Conventional Single- and Two-Phase Cooling Systems for an Electric Vehicle IGBT Power Module. *IEEE Trans. Power Electron.* **2019**, *34*, 4185–4194. [CrossRef]

62. Broughton, J.; Smet, V.; Tummala, R.R.; Joshi, Y.K. Review of Thermal Packaging Technologies for Automotive Power Electronics for Traction Purposes. *J. Electron. Packag. Trans. ASME* **2018**, *140*, 040801. [CrossRef]

63. Zhang, C.; Liu, X.; Li, J.; Song, G.; Ye, H. Simulation Study on Thermal Mechanical Properties of Different Embedded Packaging Structures and Materials of GaN Devices. In Proceedings of the 2020 21st International Conference on Electronic Packaging Technology (ICEPT), Guangzhou, China, 12–15 August 2020; pp. 1–5.

64. Lu, S.; Burgos, R.; Lu, G.-Q. Packaging and High-Temperature Characterization of a 650 V, 150 A eGaN HEMT. *Semicond. Sci. Technol.* **2021**, *36*, 034006. [CrossRef]

65. Suganuma, K. WBG Power Semiconductor Packaging with Advanced Interconnection Technologies. In Proceedings of the CIPS 2020; 11th International Conference on Integrated Power Electronics Systems, Berlin, Germany, 24–26 March 2020; pp. 168–172.

66. Chinthavali, M.S. Gas Cooled Traction Drive Inverter. U.S. Patent 9,320,179, 3 September 2013.

67. Zhang, C.-N.; Guo, F.-L.; Dong, Y.-G. Oil-Water Composite Cooling Method of Hub Motor for Electric Vehicles. In Proceedings of the 2nd International Conference on Electrical and Electronic Engineering (EEE 2019), Hangzhou, China, 26–27 May 2019; pp. 124–128. [CrossRef]

68. Pires, I.A.; Silva, R.A.; Pereira, I.T.O.; Faria, O.A.; Maia, T.A.C.; Filho, B.D.J.C. An Assessment of Immersion Cooling for Power Electronics: An Oil Volume Case Study. *IEEE Trans. Ind. Appl.* **2020**, *56*, 3231–3237. [CrossRef]

69. Yang, C.; Wang, H.; Niu, X.; Zhang, J.; Yan, Y. Design and Analysis of Cycling Oil Cooling in Driving Motors for Electric Vehicle Application. In Proceedings of the 2016 IEEE Vehicle Power and Propulsion Conference (VPPC), Hangzhou, China, 17–20 October 2016; pp. 1–6. [CrossRef]

70. Lim, D.H.; Kim, S.C. Thermal Performance of Oil Spray Cooling System for In-Wheel Motor in Electric Vehicles. *Appl. Therm. Eng.* **2014**, *63*, 577–587. [CrossRef]

71. Mademlis, G.; Orbay, R.; Liu, Y.; Sharma, N. Designing Thermally Uniform Heatsink with Rectangular Pins for High-Power Automotive SiC Inverters. In Proceedings of the IECON 2020 The 46th Annual Conference of the IEEE Industrial Electronics Society, Singapore, 18–21 October 2020; pp. 1317–1322. [CrossRef]

72. McPherson, B.; McGee, B.; Simco, D.; Olejniczak, K.; Passmore, B. Direct Liquid Cooling of High Performance Silicon Carbide (SiC) Power Modules. In Proceedings of the 2017 IEEE International Workshop On Integrated Power Packaging (IWIPP), Delft, The Netherlands, 5–7 April 2017; pp. 1–5. [CrossRef]

73. Uhlemann, A.; Hymon, E. Directly Cooled HybridPACK Power Modules with Ribbon Bonded Cooling Structures. In Proceedings of the PCIM Europe 2018; International Exhibition and Conference for Power Electronics, Intelligent Motion, Renewable Energy and Energy Management, Nuremberg, Germany, 5–7 June 2018; pp. 1–6.

74. Wang, Y.; Dai, X.; Liu, G.; Wu, Y.; Li, D.; Jones, S. Integrated Liquid Cooling Automotive IGBT Module for High Temperatures Coolant Application. In Proceedings of the PCIM Europe 2015; International Exhibition and Conference for Power Electronics, Intelligent Motion, Renewable Energy and Energy Management, Nuremberg, Germany, 19–20 May 2015; pp. 1197–1203.

75. Vangaveti, U.; Pradeep, K.T.; John, M. Thermal Behavior of the High Power Automotive Dual Sided Cooled Module. In Proceedings of the PCIM Europe 2019; International Exhibition and Conference for Power Electronics, Intelligent Motion, Renewable Energy and Energy Management, Nuremberg, Germany, 7–9 May 2019; pp. 1–6.

76. Hirao, T.; Onishi, M.; Yasuda, Y.; Namba, A.; Nakatsu, K. EV Traction Inverter Employing Double-Sided Direct-Cooling Technology with SiC Power Device. In Proceedings of the 2018 International Power Electronics Conference (IPEC-Niigata 2018-ECCE Asia), Niigata, Japan, 20–24 May 2018; pp. 2082–2085. [CrossRef]

77. Solomon, A.K.; Castellazzi, A.; Delmonte, N.; Cova, P. Highly Integrated Low-Inductive Power Switches Using Double-Etched Substrates with Through-Hole Vias. In Proceedings of the 2015 IEEE 27th International Symposium on Power Semiconductor Devices & IC's (ISPSD), Hong Kong, China, 10–14 May 2015; pp. 329–332. [CrossRef]

78. Zhu, S.; Li, Y.; Wang, Y.; Ma, Y.; Wu, C.; Jiao, M.; Zhao, Z.; Yu, J. Advanced Double Sided Cooling IGBT Module and Power Control Unit Development. In Proceedings of the 2017 IEEE International Workshop On Integrated Power Packaging (IWIPP), Delft, The Netherlands, 5–7 April 2017; pp. 1–4. [CrossRef]

79. Laloya, E.; Lucía, Ó.; Sarnago, H.; Burdío, J.M. Heat Management in Power Converters: From State of the Art to Future Ultrahigh Efficiency Systems. *IEEE Trans. Power Electron.* **2016**, *31*, 7896–7908. [CrossRef]

80. Hoque, M.J.; Günay, A.; Stillwell, A.; Gurumukhi, Y.; Pilawa-Podgurski, R.; Miljkovic, N. Modular Heat Sinks for Enhanced Thermal Management of Electronics. *J. Electron. Packag.* **2021**, *143*, 020903. [CrossRef]

81. Foulkes, T.; Oh, J.; Birbarah, P.; Neely, J.; Miljkovic, N.; Pilawa-Podgurski, R.C.N. Active Hot Spot Cooling of GaN Transistors With Electric Field Enhanced Jumping Droplet Condensation. In Proceedings of the 2017 IEEE Applied Power Electronics Conference and Exposition (APEC), Tampa, FL, USA, 26–30 March 2017; pp. 912–918. [CrossRef]

82. Jones-Jackson, S.; Rodriguez, R.; Emadi, A. Jet Impingement Cooling in Power Electronics for Electrified Automotive Transportation: Current Status and Future Trends. *IEEE Trans. Power Electron.* **2021**, *36*, 10420–10435. [CrossRef]

83. Birbarah, P.; Gebrael, T.; Foulkes, T.; Stillwell, A.; Moore, A.; Pilawa-Podgurski, R.; Miljkovic, N. Water Immersion Cooling of High Power Density Electronics. *Int. J. Heat Mass Transf.* **2020**, *147*, 118918. [CrossRef]

84. Kuncoro, I.W.; Pambudi, N.A.; Biddinika, M.K.; Widiastuti, I.; Hijriawan, M.; Wibowo, K.M. Immersion Cooling as the next Technology for Data Center Cooling: A Review. *J. Phys. Conf. Series* **2019**, *1402*, 044057. [CrossRef]

85. Chowdhury, S.; Gurpinar, E.; Su, G.-J.; Raminosoa, T.; Burress, T.A.; Ozpineci, B. Enabling Technologies for Compact Integrated Electric Drives for Automotive Traction Applications. In Proceedings of the 2019 IEEE Transportation Electrification Conference and Expo (ITEC), Detroit, MI, USA, 19–21 June 2019; pp. 1–8. [CrossRef]

86. Hensler, A.; Bidl, T.; Neugebauer, S.; Pfefferlein, S. Air Cooled SiC Three Level Inverter with High Power Density for Industrial Applications. In Proceedings of the PCIM Europe 2017; International Exhibition and Conference for Power Electronics, Intelligent Motion, Renewable Energy and Energy Management, Nuremberg, Germany, 16–18 May 2017; pp. 204–211.

87. Liu, T.; Huang, Z.; Tan, Y.; Chen, C.; Zou, K.; Peng, H.; Kang, Y.; Luo, F. A High Power Density and High Efficiency Three Phase Inverter Based on a Hybrid 3D SiC Packaging Power Module. In Proceedings of the 2018 IEEE Energy Conversion Congress and Exposition (ECCE), Portland, OR, USA, 23–27 September 2018; pp. 1944–1948. [CrossRef]

88. Li, Y.; Zhang, Y.; Yuan, X.; Zhang, L.; Ye, F.; Li, Z.; Li, Y.; Xu, Y.; Wang, Z. A 500kW Forced-Air-Cooled Silicon Carbide (SiC) 3-Phase DC/AC Converter with a Power Density of 1.246MW/m3 and Efficiency >98.5%. *IEEE Trans. Ind. Appl.* **2021**. [CrossRef]

89. Wang, Z.; Chinthavali, M.; Campbell, S.L.; Wu, T.; Ozpineci, B. A 50-KW Air-Cooled SiC Inverter with 3-D Printing Enabled Power Module Packaging Structure and Genetic Algorithm Optimized Heatsinks. *Trans. Ind. Appl.* **2019**, *55*, 6256–6265. [CrossRef]

90. Uhlemann, A.; Herbrandt, A. A New Base Plate Concept on the Basis of Aluminium-Copper Clad Materials. In Proceedings of the PCIM Europe 2012 Conference, Nuremberg, Germany, 8–10 May 2012; pp. 680–685.

91. Yin, S.; Tseng, K.J.; Zhao, J. Design of AlN-Based Micro-Channel Heat Sink in Direct Bond Copper for Power Electronics Packaging. *Appl. Therm. Eng.* **2013**, *52*, 120–129. [CrossRef]

92. Möller, S.; Karimi, D.; Vanegas, O.; el Baghdadi, M.; Kospach, A.; Lis, A.; Rabl, B.; Hegazy, O.; Abart, C. Application Considerations for Double Sided Cooled Modules in Automotive Environment. In Proceedings of the CIPS 2020; 11th International Conference on Integrated Power Electronics Systems, Berlin, Germany, 24–26 March 2020; pp. 428–434.

93. Mademlis, G.; Orbay, R.; Liu, Y.; Sharma, N.; Arvidsson, R.; Thiringer, T. Multidisciplinary Cooling Design Tool for Electric Vehicle SiC Inverters Utilizing Transient 3D-CFD Computations. *eTransportation* **2021**, *7*, 100092. [CrossRef]

94. Olejniczak, K.; Flint, T.; Simco, D.; Storkov, S.; McGee, B.; Shaw, R.; Passmore, B.; George, K.; Curbow, A.; McNutt, T. A Compact 110 KVA, 140 °C Ambient, 105 °C Liquid Cooled, All-SiC Inverter for Electric Vehicle Traction Drives. In Proceedings of the 2017 IEEE Applied Power Electronics Conference and Exposition (APEC), Tampa, FL, USA, 26–30 March 2017; pp. 735–742. [CrossRef]

95. Qi, F.; Wang, M.; Xu, L. Investigation and Review of Challenges in a High-Temperature 30-KVA Three-Phase Inverter Using SiC MOSFETs. *IEEE Trans. Ind. Appl.* **2018**, *54*, 2483–2491. [CrossRef]

96. Zhang, C.; Srdic, S.; Lukic, S.; Kang, Y.; Choi, E.; Tafti, E. A SiC-Based 100 KW High-Power-Density (34 KW/L) Electric Vehicle Traction Inverter. In Proceedings of the 2018 IEEE Energy Conversion Congress and Exposition (ECCE), Portland, OR, USA, 23–27 September 2018; pp. 3880–3885. [CrossRef]

97. Gurpinar, E.; Wiles, R.; Zhou, F.; Liu, Y.; Dede, E.M. SiC MOSFET-Based Power Module Design and Analysis for EV Traction Systems. In Proceedings of the 2018 IEEE Energy Conversion Congress and Exposition (ECCE), Portland, OR, USA, 23–27 September 2018; pp. 1722–1727. [CrossRef]

98. Huber, T.; Kleimaier, A. Novel SiC Module Design—Optimised for Low Switching Losses, Efficient Cooling Path and Low Inductance. In Proceedings of the CIPS 2018 10th International Conference on Integrated Power Electronics Systems, Stuttgart, Germany, 20–22 March 2018; pp. 571–576.

99. Becker, N.; Bulovic, S.; Bittner, R.; Herzer, R. Thermal Simulation for Power Density Optimization of SiC-MOSFET Automotive Inverter. In Proceedings of the CIPS 2020; 11th International Conference on Integrated Power Electronics Systems, Berlin, Germany, 24–26 March 2020; pp. 1–6.

100. Liu, C.-K.; Wu, S.-T.; Lo, Y.-Y.; Chiu, P.-K.; Lin, H.-H.; Chen, Y.-S.; Tzeng, C.-M. Double-Sided Cooling SiC Power Module Packaging for Industrial Motor Driving System. In Proceedings of the 2020 15th International Microsystems, Packaging, Assembly and Circuits Technology Conference (IMPACT), Taipei, Taiwan, 21–23 October 2020; pp. 105–108. [CrossRef]

101. Tang, G.; Wai, L.C.; Boon Lim, S.; Lau, B.L.; Kazunori, Y.; Zhang, X.W. Thermal Analysis, Characterization and and Material Selection for SiC Device Based Intelligent Power Module (IPM). In Proceedings of the 2020 IEEE 70th Electronic Components and Technology Conference (ECTC), Orlando, FL, USA, 3–30 June 2020; pp. 2078–2085. [CrossRef]

102. Lee, J.; Ki, S.; Seo, D.; Kim, J.; Nam, Y. Liquid Cooling Module Incorporating a Metal Foam and Fin Hybrid Structure for High Power Insulated Gate Bipolar Transistors (IGBTs). *Appl. Therm. Eng.* **2020**, *173*, 115230. [CrossRef]

103. Takai, K.; Yuki, K.; Yuki, K.; Kibushi, R.; Unno, N. Heat Transfer Performance of Uni-Directional Porous Heat Sink for Cooling of next Generation on-Vehicle Inverter. In Proceedings of the 2017 International Conference on Electronics Packaging (ICEP), Yamagata, Japan, 19–22 April 2017; pp. 181–187. [CrossRef]

104. Cheng, C.C.; Chang, P.C.; Li, H.C.; Hsu, F.I. Design of a Single-Phase Immersion Cooling System through Experimental and Numerical Analysis. *Int. J. Heat Mass Transf.* **2020**, *160*, 120203. [CrossRef]

105. Singh, R. Vehicle Thermal Management Using Heat Pipes. In Proceedings of the 2019 IEEE CPMT Symposium Japan (ICSJ), Kyoto, Japan, 18–20 November 2019; pp. 75–78. [CrossRef]

106. Mochizuki, M. Latest Development and Application of Heat Pipes for Electronics and Automotive. In Proceedings of the 2017 IEEE CPMT Symposium Japan, Kyoto, Japan, 20–22 November 2017; pp. 87–90. [CrossRef]

107. Shafahi, M.; Bianco, V.; Vafai, K.; Manca, O. An Investigation of the Thermal Performance of Cylindrical Heat Pipes Using Nanofluids. *Int. J. Heat Mass Transf.* **2010**, *53*, 376–383. [CrossRef]

108. Gupta, K.; da Silva, C.; Nasr, M.; Assadi, A.; Matsumoto, H.; Trescases, O.; Amon, C.H. Thermal Management Strategies for a High-Frequency, Bi-Directional, On-Board Electric Vehicle Charger. In Proceedings of the 2018 17th IEEE Intersociety Conference on Thermal and Thermomechanical Phenomena in Electronic Systems (ITherm), IEEE, San Diego, CA, USA, 29 May–1 June 2018; pp. 935–943. [CrossRef]

109. Chang, Y.; Sajjad Bahman, A.; Luo, H.; Li, W.; He, X.; Iannuzzo, F.; Blaabjerg, F. A Busbar Integrated SiC-Based Converter with Embedded Heat-Pipes. In Proceedings of the 2019 10th International Conference on Power Electronics and ECCE Asia (ICPE 2019—ECCE Asia), Busan, Korea, 27–30 May 2019; pp. 2166–2172. [CrossRef]

110. Yuki, K.; Kibushi, R.; Tsuji, R.; Takai, K.; Unno, N.; Ogushi, T.; Murakami, M.; Numata, T.; Nomura, H.; Ide, T. Thermal Management of Automotive Sic-Based on-Board Inverter with 500 w/cm^2 in Heat Flux, and Two-Phase Immersion Cooling by Breathing Phenomenon Spontaneously Induced by Lotus Porous Copper Jointed onto a Grooved Heat Transfer Surface. *J. Therm. Sci. Technol.* **2020**, *15*, 1–11. [CrossRef]

111. Lee, W.; Li, S.; Han, D.; Sarlioglu, B.; Minav, T.A.; Pietola, M. A Review of Integrated Motor Drive and Wide-Bandgap Power Electronics for High-Performance Electro-Hydrostatic Actuators. *IEEE Trans. Transp. Electrif.* **2018**, *4*, 684–693. [CrossRef]

112. Dai, H.; Torres, R.A.; Lee, W.; Jahns, T.M.; Sarlioglu, B. Integrated Motor Drive Using Soft-Switching Current-Source Inverters with SiC- and GaN-Based Bidirectional Switches. In Proceedings of the 2020 IEEE Energy Conversion Congress and Exposition (ECCE), Detroit, MI, USA, 11–15 October 2020; pp. 2372–2378. [CrossRef]

113. Lee, W.; Sarlioglu, B. Thermal Analysis of Lateral GaN HEMT Devices for High Power Density Integrated Motor Drives Considering the Effect of PCB Layout and Parasitic Parameters. In Proceedings of the 2018 IEEE Transportation Electrification Conference and Expo (ITEC), Long Beach, CA, USA, 13–15 June 2018; pp. 471–476. [CrossRef]

114. Fukuda, K.; Akatsu, K. 5-Phase Double Winding PMSM with Integrated SiC Inverter for In-Wheel Motor. In Proceedings of the 2019 22nd International Conference on Electrical Machines and Systems (ICEMS), Harbin, China, 11–14 August 2019; pp. 1–5.

115. Wu, Z.; Zhang, Y.; Han, P.; Chen, C.; Kang, Y. GaN HEMT Based High Power Density Integrated Inverter for a Six-Phase Permanent Magnet Synchronous Motor without Forced Convection. In Proceedings of the PCIM Europe, Nuremberg, Germany, 11–14 August 2019; pp. 1105–1109. [CrossRef]